Journal of Power Sources, 43–44 (1993) 111–118

Modeling the discharge behavior of the lithium/iodine battery

Paul M. Skarstad and Craig L. Schmidt
Medtronic, Inc., 6700 Shingle Creek Parkway, Minneapolis, MN 55430 (USA)

Abstract

We have previously reported the development of a physically-based mode describing the discharge behaviour of the lithium/iodine battery. Values for the parameters of the model have been determined through analysis of discharge data from a wide variety of battery designs. This paper reviews the essential features of the model and describes several applications. These applications include estimation of performance distributions through Monte-Carlo simulations, analysis of variability in discharge performances, and identification of the parameters to which discharge performance is most sensitive.

Introduction

The lithium/iodine battery is the most successfully commercialized solid-electrolyte battery. It was introduced as a power source for implanted cardiac pacemakers twenty years ago [1], and the high reliability, high energy density and manufacturability of the system have made it the most frequently used power source for this application. The cathode of this battery consists of a two-phase mixture of crystalline iodine and a viscous solution of iodine and poly(2-vinylpyridine). When the battery is constructed, the lithium and molten cathode material are placed directly in contact. The discharge product, lithium iodide, forms the electrolyte *in situ* as the battery discharges.

The general structure and principles of lithium/iodine batteries have been described in reviews [2, 3]. Only recently have the mechanisms of voltage polarization under load been discussed in quantitative terms [4]. There are several keys to understanding the polarization behavior of the lithium/iodine battery:

(i) Recognition of the battery as a collection of bulk resistors and interfaces in series. On this basis the total impedance is expected to be a sum of ohmic terms corresponding to the bulk resistors and non-ohmic corresponding to interfacial processes.

(ii) Separation of ohmic and non-ohmic polarization by analysis of complex impedance data. Complex-plane plots of impedance for batteries under load show a current-independent real intercept at intermediate frequencies and current-dependent features at low frequencies.

(iii) Separation of electrolyte- and cathode-related components of the ohmic resistance. These two components have different dependencies on discharged capacity and work together to give discharge curves of lithium/iodine batteries their characteristic shape.

(iv) Demonstration that discharge-dependence of non-ohmic polarization, comprised of activation overpotential and concentration polarization, can in most cases be adequately described by a single three-parameter logarithmic function of discharged capacity.

Elsevier Sequoia

(v) Establishment of the thermodynamic framework of the system through measurement of open-circuit potentials as a function of cathode composition. This work has identified the boundary between two-phase and single-phase cathode composition, the limiting cathode composition, and the functional form of the loss in open-circuit potential which occurs in the single-phase region of cathode composition.

Quantitative understanding of the processes which lead to voltage loss under load has allowed the development of a physically-based mathematical model of the steady-state discharge of lithium/iodine batteries. This model allows the load voltage of a lithium/iodine cell to be calculated in terms of the application current and three-parameter characteristic of the battery design: anode area, cathode capacity and initial cathode composition.

In addition to prediction of mean behavior, the steady-state model has allowed prediction of the distribution of mean behavior via Monte Carlo simulation, based on the distributions of design-independent parameters of the model observed over a wide range of battery designs.

Summary of the steady-state discharge model

The essential features of the lithium/iodine battery model are illustrated in Table 1. The model describes the loss of voltage during discharge in terms of five physical processes: ohmic resistance of electrolyte, ohmic resistance of cathode, charge-transfer polarization, concentration polarization, and decrease in open-circuit potential.

Figure 1 shows ohmic and non-ohmic components of resistance as functions of discharged capacity for a typical lithium/iodine battery. Changes in the electrolyte component of ohmic resistance dominate much of the early discharge history. Electrolyte resistance is observed to vary exponentially with depth-of-discharge as shown in Fig. 1. The parameters of the exponential function used to model the electrolyte resistance (B and β in Table 1) are normalized by anode area.

The electrolyte consists of a layer of lithium iodide of ever-increasing thickness as the cell discharges. Dense planar growth of electrolyte has been shown to lead to a linear relation between resistance and capacity discharged. However, practical batteries are made with a coating of poly(2-vinylpyridine) on the anode. This coating has been shown to break down to yield a small amount of liquid electrolyte wetting the lithium

TABLE 1

Summary of model[a]

	Ohmic		Non-ohmic		Loss of OCV
Source	Electrolyte	Cathode	Charge-transfer polarization	Concentration polarization	
Determining factors	Q, Area	Cathode-composition, geometry	Cathode-composition, I, Area	I/Area	Cathode-composition
Adjustable parameters	B_{el}, β_{el}	ρ_0, κ, γ	α, K, γ	M	γ

[a]Fixed parameters from open-circuit voltage data: limiting cathode composition (r_1), cathode composition at phase-boundary (r_{pb}), and effective value of 'n' in Nernst equation.

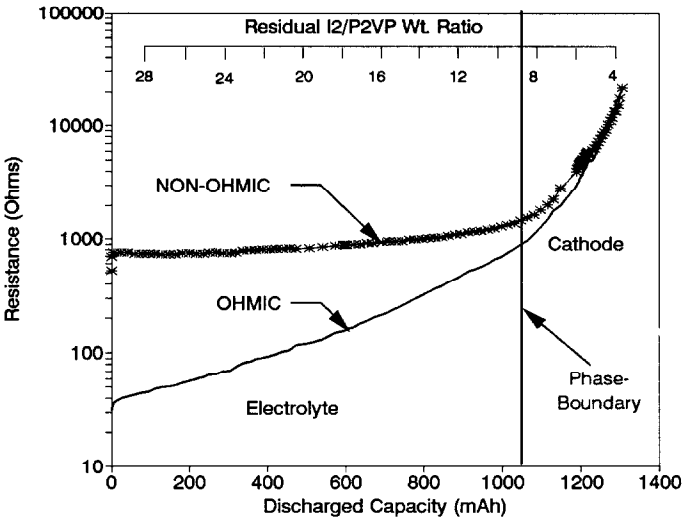

Fig. 1. Ohmic and non-ohmic resistance for a typical lithium/iodine battery. Region of ohmic resistance dominated by electrolyte and by cathode are indicated. Anode area: 10.9 cm^2; stoichiometric cathode capacity: 1.53 A h; starting cathode composition: 30 parts I_2 per part poly(2-vinylpyridine) (P_2VP) by weight, and discharge rate: 19 μA.

iodide discharge product, reducing the resistance of the electrolyte and changing the shape of the discharge curve to the exponential relation seen in Fig. 1 [5].

The cathode resistance is relatively small and varies little while the composition of the cathode is two phase. However, once the cathode reaches its single-phase composition, the resistance of the cathode increases rapidly and soon dominates the total resistance of the cell. It is the shift from electrolyte dominance to cathode dominance of the ohmic resistance that yields the characteristic 'knee' in the discharge curve near end-of-service.

The cathode resistance in the single-phase region has been shown to be separable into a geometric factor and a resistivity. The resistivity shown in Fig. 2 varies exponentially with cathode composition (parameters ρ_0 and κ in Table 1). A satisfactory geometric factor for prediction of cathode resistance is the volume of the cathode at the boundary between the two-phase and one-phase regions divided by the square of the area of the anode. The cathode in the single-phase region increases in resistance exponentially as iodine is removed. The apparent viscosity of the cathode material also increases as iodine is removed, and the material goes from being fluid at the phase boundary to glassy at end-of-service. We are unable to account for the exponential dependence of cathode resistance on composition at this point. However, similar behavior has been observed for halide salts dissolved in inorganic glasses [6].

In the non-ohmic component of resistance both kinetic and mass-transfer effects are important. In the two-phase region of cathode composition, the non-ohmic resistance varies little (Fig. 1) and has been taken to be constant at a given current. For the single-phase region, an expression for the polarization resistance as a function of cathode composition and current density has been derived from the cathodic branch of the current–voltage relation for heterogeneous kinetics. The result is a three-parameter logarithmic function in discharged capacity which has been shown to fit

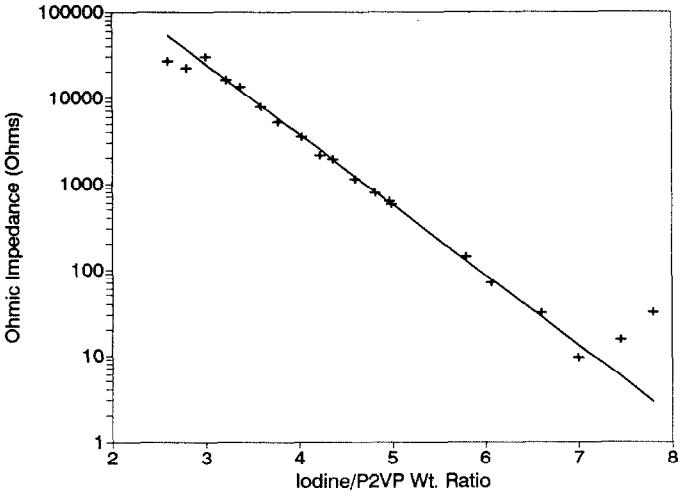

Fig. 2. Resistance as a function of composition for iodine/poly(2-vinylpyridine) (P_2VP) cathode material.

and predict the non-ohmic impedance well. From the three parameters, a transfer coefficient, a mass-transfer coefficient, and a heterogeneous rate constant have been obtained (α, M, and K, respectively in Table 1). Finally, a cathode availability factor (γ) is included; this is found to vary little over a wide range of designs.

The nine design-independent parameters described above have been evaluated for data from at least 15 different implantable battery designs varying widely in electrode loading and cathode composition, leading to average values and standard deviations for each parameter. Additionally, the model requires four fixed thermodynamic parameters: the open-circuit potential in the two-phase region of cathode composition, the phase-boundary composition of the cathode, the limiting cathode composition, and the effective value of 'n' in the Nernst equation. These have been experimentally determined through evaluation of open-circuit voltage data as a function of cathode composition.

Applications of the model

Simulation of performance distributions

The mean values of the design-independent parameters can be used to calculate the expected value of the load voltage as a function of discharge for a battery design. This information is of great value in designing a battery for a specific application. However, in order to fully assess the applicability of a battery design, some knowledge of its expected performance distribution is also necessary. This can be obtained from the distributions of parameter values of the model via Monte Carlo simulation. Simulations were carried out using the Lotus 1-2-3 (Lotus Development Corporation) add-on program at risk (Palisade Corporation, Newfield, NY).

One important characteristic of lithium/iodine batteries in implantable medical applications is the rate of voltage decline at end-of-service. Figure 3 shows mean discharge curves near end-of-service for several groups of batteries of the design

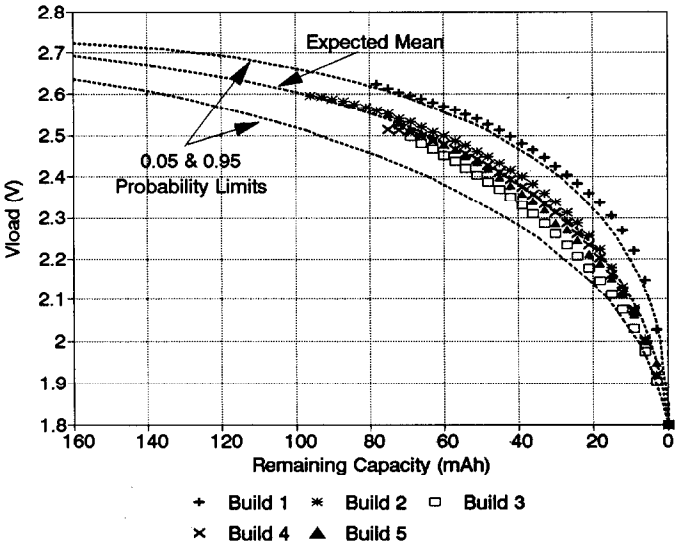

Fig. 3. Shape of lithium/iodine battery discharge curve near end-of-service. Cell described in Fig. 1.

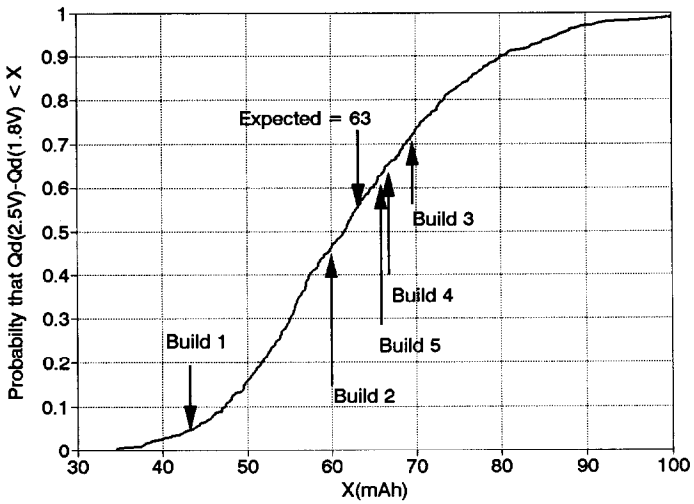

Fig. 4. Distribution function for capacity delivered in voltage interval 2.5 to 1.8 V. Cell described in Fig. 1.

described in Fig. 1. The curves have been translated on the capacity scale to that they are coincident at 1.8 V, the end-of-service point; 5 and 95% confidence limits are indicated. Figure 4 shows the distribution function for capacity between 2.5 and 1.8 V at 19 μA obtained from the simulations. In both Figs. 3 and 4 an outlying group of batteries is apparent. The probability of such an event is quantified by the distribution function in Fig. 4.

TABLE 2

Comparison of model parameters of batteries in Fig. 3 to overall average parameters

	Electrolyte		Cathode		Non-ohmic	
	β_{el} (cm^2/A h)	B_{el} (kΩ cm^2)	κ (kΩ cm^2)	ρ (kΩ cm)	α	K 10^4 (mA/cm^2)
Group 1	34.1	0.26	1.12	4400	0.36	6.3
Average of group 2–5	32.3	0.61	0.95	4700	0.28	4.2
Model average	27.8	0.62	0.93	5070	0.31	3.8
Model standard deviation	4.5	0.22	0.19	910	0.03	1.1

Analysis of discharge data

Using a physically-based model to characterize and compare two or more sets of discharge data can provide insight into the underlying source of variation. For example, the discharge data from each battery group in Figs. 3 and 4 were fit to the discharge model described earlier. The values of the design-independent variables obtained for the four similar groups (groups 2–5) were averaged and compared with the values determined for group 1. The results of this analysis are shown in Table 2 along with the overall average parameter values obtained from analyses of about 15 different battery designs.

The cathode parameters, ρ_0 and κ, obtained for group 1 are nearly identical to average of the four similar groups and the overall average. Thus, it is unlikely that the observed difference in discharge behavior can be attributed to variation in the cathode material or cathode processing. However, one of the electrolyte parameters (B_{el}) and two of non-ohmic resistance parameters (α and K) determined for group 1 differ significantly from the average of groups 2–5 and the overall average. While this level of analysis does not identify a specific source of the variation in discharge performance, it does eliminate certain sources and provides a general direction for future experimental work.

Sensitivity analysis

As pointed out earlier, the distribution of parameter values obtained through analysis of discharge data result in a relatively wide range of possible discharge performances. It is of interest to know to what extent the variability associated with each parameter affects the overall discharge performance. This knowledge can provide additional focus for experimental work.

Sensitivity analyses were carried out using a 12-run Plackett-Burman experimental design. The high value used for each parameter was its mean plus one standard deviation, and the low value was its mean minus one standard deviation. The measured response was the capacity between two voltages in the end-of-service region at a given discharge rate. This is a simple but useful means of characterizing the shape of the discharge curve in this region.

Figure 5 summarizes the results of such an analysis performed on the battery design described in Fig. 1. The measured response was the capacity between 2.55 and 1.80 V at a discharge rate of 20 μA. The mean capacity between these two voltages was calculated to be 88 mA h. The ordinate in Fig. 5 is the average effect of each

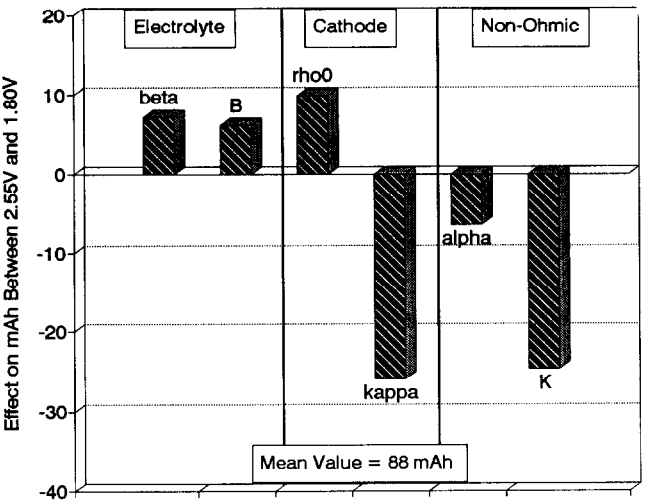

Fig. 5. Sensitivity of end-of-service interval to parameter variation.

parameter in this interval. A negative effect denotes that a large value of the parameters yields a shorter end-of-service interval than a small value.

The mass-transfer parameter, M, and the cathode availability factor, γ, have virtually no effect on the shape of the discharge curve regardless of battery design. These parameters have been excluded from Fig. 5.

The variation of the electrolyte parameters, B_{el} and β_{el} have a relatively small effect on the end-of-service in this case. This results from the fact that the electrolyte resistance in this region is relatively small with respect to the cathode resistance and non-ohmic resistance. Thus, variation of the electrolyte parameters have little influence on the end-of-service characteristics. The most significant effects results from variation in one of the cathode parameters (κ) and one of the non-ohmic parameters (K). When this knowledge is added to the analysis of the discharge data discussed above, it becomes apparent that the aberrant behavior of group 1 in Figs. 3 and 4 is primarily associated with variation of the non-ohmic parameter, K. Again, this analysis does not identify a specific cause of the variation, but it does provide improved focus for additional experimental work.

Additional sensitivity analyses have shown that the model parameters which have the greatest influence on discharge performance are a function of battery design. As the cathode loading per unit anode area increases, the end-of-service interval becomes more sensitive to variation in the electrolyte parameters and less sensitive to variation in cathode and non-ohmic parameters.

Conclusion

A model of the discharge behavior of lithium/iodine batteries has been developed which accurately predicts voltage as a function of discharged capacity and current. The distribution function of any quantity derivable from the voltage curve, e.g., capacity to a cutoff voltage or capacity within a voltage window, can be simulated based on the distributions of parameters of the model. Development of the model has given

insight into the mechanisms of polarization in the lithium/iodine battery and has provided a means of focusing research efforts.

Two important relations within the model are empirical: (i) the exponential resistance of electrolyte as a function of discharged capacity, and (ii) the exponential resistivity of the cathode as a function of cathode composition. Further study is needed to understand these relations fully.

References

1 W. Greatbatch, J. H. Lee, W. Mathias, M. Eldridge, J. R. Moser and A. A. Schneider, *IEEE Trans. Biomed. Eng., 18* (1971) 317.
2 B. B. Owens, P. M. Skarstad and D. F. Untereker, in D. Linden (ed.), *Handbook of Batteries and Fuel Cells,* McGraw-Hill, New York, 1984, Ch. 12, pp. 9–21.
3 C. F. Holmes, in B. B. Owens (ed.), *Batteries of Implantable Biomedical Devices,* Plenum, New York, 1986, pp. 133–180.
4 C. L. Schmidt and P. M. Skarstad, in T. Keily and B. W. Baxter (eds.), *Power Sources, 13,* International Power Sources Committee, Leatherhead, UK, 1991, pp. 347–361.
5 J. B. Phipps, T. G. Hayes, P. M. Skarstad and D. F. Untereker, *Solid State Ionics, 18–19* (1986) 1073–1077.
6 A. Kone and J. L. Souquet, *Solid State Ionics, 18–19* (1986) 454–460.